Effects of Reactive Low-Profile Additives on the Properties of Cured Unsaturated Polyester Resins. I. Volume Shrinkage and Internal Pigmentability

Jyh-Ping Dong, Jeng-Huei Lee, Duen-Horng Lai, Yan-Jyi Huang

Department of Chemical Engineering, National Taiwan University of Science and Technology, Taipei, Taiwan 106, Republic of China

Received 30 March 2004; accepted 15 December 2004
DOI 10.1002/app.21813
Published online in Wiley InterScience (www.interscience.wiley.com).

ABSTRACT: The effects of reactive poly(methyl methacrylate) (PMMA) and poly(vinyl acetate)-*block*-PMMA as low-profile additives (LPAs) on the volume shrinkage characteristics and internal pigmentability for low-shrink unsaturated polyester (UP) resins during curing at 110°C were investigated. These reactive LPAs, which contained peroxide linkages in their backbones, were synthesized by suspension polymerization with polymeric peroxides as initiators. Depending on the LPA composition and molecular weight, the reactive LPAs led to a considerable volume reduction or even to a volume expansion after the curing of styrene (ST)/UP/LPA ternary systems; this was attributed mainly to the expansion effects of the LPAs on the ST-crosslinked polyester microgel structures caused by the reduction in the cyclization reaction of the UP resin during curing as well as to the repulsive forces between the chain segments of UP and LPAs within the microgel structures. The experimental results were explained by an integrated approach of measurements for the static phase characteristics of the ST/UP/LPA system, reaction kinetics, cured sample morphology, and microvoid formation with differential scanning calorimetry, scanning electron microscopy, optical microscopy, and image analysis. With the aid of the Takayanagi mechanical model, the factors leading to both a good volume shrinkage control and acceptable internal pigmentability for the molded parts were also explored. © 2005 Wiley Periodicals, Inc. J Appl Polym Sci 98: 264–275, 2005

Key words: additives; polyesters; resins

INTRODUCTION

Unsaturated polyester (UP) resins are usually made from maleic anhydride (MA), saturated dicarboxylic acid or its anhydride, and glycol by polycondensation reactions. The number of C═C unsaturations along the UP backbone generally ranges from 4 to 20, with a corresponding number-average molecular weight (M_n) of 800 to 5000 for the UP. The UP resins can be copolymerized with styrene (ST) monomers via free-radical crosslinking reactions to form a three-dimensional network. However, one of the major problems in the reactive processing of UP molding compounds, such as sheet molding compound and bulk molding compound, is the high polymerization shrinkage. In general, a 7–10% volume shrinkage may result,[1] which in our opinion, is due to the extensive intramolecular or cyc1ization reactions of UP molecules and the formation of compact microgel structures during curing.[2] This is in contrast to a cure shrinkage of usually less than 2% for epoxy resin,[3] which possesses epoxy groups at the chain ends instead of along the chain, so intramolecular crosslinking reactions are considerably reduced during the curing process. Also, the ring-opening of epoxy groups during curing may facilitate local volume expansion and, in turn, can greatly compensate for polymerization shrinkage.

For the past 35 years, the sheet molding compound and bulk molding compound industries have used the approach of adding specific thermoplastic polymers as low-profile additives (LPAs) in UP resins to reduce or even eliminate polymerization shrinkage during the curing process.[1,4] Most studies[1,4–13] have been devoted to the use of nonreactive LPAs, such as thermoplastic polyurethane, poly(vinyl acetate) (PVAc), poly(methyl methacrylate) (PMMA), and polystyrene (PS), and have been aimed at the compensation of volume shrinkage by effective microvoid and/or microcrack formation[5,6] during curing rather than at the minimization of intrinsic polymerization shrinkage (i.e., the minimization of intramolecular or cyclization reactions of UP molecules during curing). Although some reactive LPAs, such as PVAc-*b*-PMMA and PVAc-*b*-PS, with many peroxide linkages along the skeleton of LPAs, have been successfully developed[14–16] to minimize the volume shrinkage of UP resins, the fundamental principles have not been treated.

Correspondence to: Y.-J. Huang (yjhuang@ch.ntust.edu.tw).
Contract grant sponsor: National Science Council of the Republic of China; contract grant number: NSC 89-2216-E-011-020.

TABLE I
Raw Materials and Reaction Temperature History Used in the Synthesis of Reactive LPAs

LPA code	MMA (g)	ST (g)	VAc (g)	ATPPO (g)[a]	CTA (g)	PVOH solution (g)[b]	Reaction temperature history (°C)
PMMA26K	50	—	—	5	0.3	400	60–70[c]
PMMA57K	50	—	—	5	0.15	400	60–70
PMMA136K	50	—	—	5	0	400	60–70
VAc-*b*-MMA18K(14)	45	—	5	5	0.27	400[d]	60–70[e]
VAc-*b*-MMA26K(17)	40	—	10	5	0.24	400	60–70
VAc-*b*-MMA38K(15)	45	—	5	5	0.135	400	60–70
VAc-*b*-MMA31K(24)	35	—	15	5	0.21	400	60–70
VAc-*b*-MMA54K(24)	40	—	10	5	0.12	400	60–70

[a] The weight ratio of ATPPO to monomer was 1 : 1
[b] The PVOH aqueous solution contained 0.5 wt % of PVOH (M_n = 88,000 g/mol), and the weight ratio of water to monomer was 8 : 1 for the reaction system.
[c] The reaction was carried out at 60°C for 3 h and then at 70°C for another 5 h.
[d] For either of the two stages of suspension polymerization, 400 g of 0.5 wt % PVOH aqueous solution was used (see text).
[e] The MMA homopolymerization was carried out at 60°C for 3 h and was followed by the VAc/MMA copolymerization at 70°C for another 5 h.

Low-profile polyester molding compounds, when formulated with pigments, usually exhibit an unacceptable hazing of the pigment's color. Recently, unique nonreactive LPAs have been developed[17] that give significantly improved deep color pigmentation and maintain a smooth surface and zero shrinkage, yet no one has dealt with the fundamental principle.

The polymerization shrinkage of ST/UP/LPA ternary systems during curing is connected with both intrinsic polymerization shrinkage and volume shrinkage compensation by microvoid formation.[11] The former factor would be greatly affected by reactive LPAs because they may participate in the crosslinking copolymerization of ST and UP during curing, leading to a variation in the compactness of microgel structures and, in turn, to the alteration of intrinsic polymerization shrinkage after curing. The objective of this study was to investigate the effects of reactive PMMA and methyl methacrylate (MMA)-based block copolymer types of LPAs on the volume shrinkage characteristics and internal pigmentability of ST/UP/LPA ternary systems. With an integrated approach combining the static ternary phase characteristics of ST/UP/LPA at 25°C, cured sample morphology, reaction kinetics, microvoid formation, and property measurements, factors leading to both good volume shrinkage control and acceptable internal pigmentability for the molded parts are discussed.

EXPERIMENTAL

Reactive LPA

The reactive PMMA and PVAc-*b*-PMMA types of LPAs were synthesized by suspension polymerization.[14,18,19] Self-synthesized polymeric peroxides (PPOs), *n*-dodecyl mercaptan (Acros, Morris Plains, N.J.), and poly(vinyl alcohol) (PVOH; M_n = 88,000 g/mol, Acros) were used as the initiator, chain-transfer agent (CTA), and suspending agent, respectively. The first series of LPAs was made from MMA (Acros), and the second series of LPAs was made from vinyl acetate (VAc; Acros) and MMA. The raw materials and reaction temperature history used in the synthesis of the eight LPAs for this study are summarized in Table I. These LPAs are reactive because there are peroxide linkages in their backbones, which are capable of thermal decomposition during curing, and may have participated in free-radical crosslinking copolymerizations for the ST/UP/LPA systems.

Synthesis of PPOs

A five-necked, 0.5-L jacketed glass reaction vessel equipped with a thermometer, a stirrer, and a water pump was used in the synthesis of PPOs. A temperature-controlled circulation water bath (Haake F3C, Karlsruhe, Germany) was also used to control the reaction temperature by water flowing through the jacket. Into the first reactor, we charged 109.8 g (0.6 mol) of adipoyl chloride (AC; Merck, Darmstadt, Germany) and 45 g (0.3 mol) of triethylene glycol (TEG; Acros). The reaction was then carried out under agitation (at a stirring speed of 400 rpm) at a reaction temperature of 50°C, and with the pressure maintained at 40–50 mmHg (to eliminate HCl for the facilitation of polymerization) for 3 h; a dark brown viscous liquid of triethylene glycol–bis(adipoyl chloride) (ATCl) was produced.

$$2ClCO(CH_2)_4COCl\ (AC) + HO(C_2H_4O)_3H\ (TEG) \rightarrow ClCO(CH_2)_4CO—[(OC_2H_4)_3OCO(CH_2)_4CO]_n—Cl\ (ATCl) + HCl \quad (1)$$

Into a second five-necked, 0.5-L jacketed glass reaction vessel, we charged 231.8 g of a 5.1 wt % aqueous solution of sodium peroxide (0.295 mol of NaOH) first. After the vessel temperature was controlled at 5°C, 12.14 g of a 35 wt % aqueous solution of hydrogen peroxide (0.125 mol of H_2O_2) was added to the reactor for the production of Na_2O_2, where a nitrogen sparge rate of 40 mL/min and a stirring speed of 450 rpm were maintained:

$$2NaOH\ (excess) + H_2O_2 \rightarrow Na_2O_2 + 2H_2O \qquad (2)$$

After 10 min of reaction time, 50 g of ATCl (0.113 mol) obtained in the previous reaction was charged into the second reaction vessel through a feeding funnel at an addition rate of 1 g/min. After completion of the feeding, the reaction was maintained at 5°C for another 30 min to complete the reaction and to produce the PPOs (ATPPOs which can be defined as a polymeric peroxide, PPO, made from adipoyl chloride, A, and triethylene glycol, T, monomers):

$$ATCl + Na_2O_2\ (excess) \rightarrow [\text{—}CO(CH_2)_4CO\text{—}((OC_2H_4)_3 OCO(CH_2)_4CO)_n\text{—}\mathbf{O}\text{—}\mathbf{O}\text{—}]_m\ (ATPPO) + NaCl \qquad (3)$$

The resultant precipitate was poured out and was then washed with water three times, filtered, and vacuum-dried at room temperature overnight. The obtained white solid was then dissolved in 2.6 times by weight of chloroform; the resultant solution was poured into 11.4 times by weight of methanol for the purification by recrystallization and was stored in a refrigerator overnight. After the separation by filtration under suction and vacuum drying at room temperature overnight in a vacuum oven, a purified ATPPO white solid was obtained.

Synthesis of reactive-PMMA-type LPAs

Into a five-necked, 2-L glass reaction vessel provided with a stirrer, a N_2 inlet, a reflux condenser, a thermocouple, and a temperature controller, we charged 400 g of a 0.5 wt % aqueous solution of PVOH and a solution that was prepared by the mixture of the monomers, CTA, and ATPPO, as shown in Table I. The reactants were mixed at room temperature for 30 min at a nitrogen sparge rate of 40 mL/min and a stirring speed of 500 rpm and were then heated to the reaction temperatures. For the MMA reaction systems, the polymerization was carried out at 60°C isothermally for 3 h and was then carried out at 70°C for another 5 h. The polymerization product was poured out and was then washed with hot water (70–80°C) three times on a hot plate with stirring to effectively remove the suspending agent adsorbed on the polymer, filtered under suction, and vacuum-dried overnight; a white granular reactive homopolymer was obtained.

Synthesis of reactive PVAc-*b*-PMMA type LPAs

For the synthesis of the reactive PVAc-*b*-PMMA types of LPA, a two-stage reaction was adopted. Monomer 1 (MMA), CTA, and ATPPO were mixed first, and the first stage of suspension polymerization was then carried out at 60°C for 3 h in a five-necked, 2-L glass reaction vessel (Table I). After purification, a PMMA homopolymer bearing peroxide linkages on its backbone was obtained.

For the second stage of reaction, 400 g of a 0.5 wt % aqueous solution of PVOH, monomer 2 (i.e., VAc), and the reactive homopolymer obtained in the first stage of the reaction, which was used as an initiator, were charged into a five-necked, 2-L glass reaction vessel (no additional ATPPO was added). After thorough mixing, the suspension polymerization was carried out at 70°C for 5 h, where the pretreatment and purification procedures were essentially the same as those used for the reactive PMMA types of LPA described previously. A random block copolymer of MMA and VAc, that is, PMMA-*b*-PVAc, was then obtained, where the PMMA segment, with peroxide linkages on it, was reactive and where the PVAc segment was nonreactive.

The properties of the reactive LPAs synthesized in this study are summarized in Table II.

UP resins

The UP resin[23] was made from MA, 1,2-propylene glycol (PG), and phthalic anhydride (PA) with a molar ratio of 0.63 : 1.01 : 0.367. The acid number and hydroxyl number were found to be 28.0 and 28.2 by end-group titration, which gave an M_n of 2000 g/mol.

Preparation of sample solutions

For the sample solution, 10 wt % LPA was added, whereas the molar ratio of ST to polyester C═C bonds was fixed at molar ratio of styrene to polyester C═C bonds (MR) = 2 : 1. The reaction was initiated by 1 wt % *tert*-butyl perbenzoate (TBPB). For the sample solution with pigments, 10 wt % Bordeaux Red was added as pigment. All the cure reactions were carried out at 110°C isothermally.

Phase characteristics

To study the compatibility of ST/UP/LPA systems before reaction, 20 g of sample solutions was prepared in 100-mL separatory glass cylinders, which were placed in a constant-temperature water bath at 25°C.

TABLE II
LPAs Used in This Study

LPA code	Monomers	Molar composition[a]	M_n[b]	M_w[b]	PD[b]	T_g (°C)[c]	—O—O— per LPA[f]
Reactive LPAs							
PMMA26K	MMA	—	26,000	80,000	3.1	96.2	—
PMMA57K	MMA	—	57,000	183,000	3.2	101.5	0.48
PMMA136K	MMA	—	136,000	220,000	1.6	100.4	2.41
VAc-b-MMA18K(14)	VAc, MMA	0.14 : 0.86	18,000	87,000	4.8	92.7	—
VAc-*b*-MMA26K(17)	VAc, MMA	0.17 : 0.83	26,000	97,000	3.7	85.2	—
VAc-*b*-MMA38K(15)	VAc, MMA	0.15 : 0.85	38,000	147,000	3.9	75.9 (46.4, 103.6)[d]	0.62
VAc-*b*-MMA31K(24)	VAc, MMA	0.24 : 0.76	31,000	124,000	4.0	65.5 (106.1)[d]	0.33
VAc-*b*-MMA54K(24)	VAc, MMA	0.24 : 0.76	54,000	212,000	3.9	94.6	0.68
Nonreactive LPAs							
PVAc109K[20]	VAc	—	109,000	166,000	1.52	20.4	
VAc–VC16K(23)[21,22]	VAc, VC[e]	0.228 : 0.772	16,100	28,300	1.76	58.2	

[a] By ^{1}H-NMR.
[b] By GPC (g/mol).
[c] By DSC.
[d] The medium transition temperature (i.e., 75.9 or 65.5°C) was the T_g for the random block copolymer of VAc and MMA, whereas the lower (i.e., 46.4°C) and higher (i.e., 103.6 or 106.1°C) transition temperatures were the T_g's for the PVAc and PMMA segments, respectively.
[e] A random copolymer of VAc and VC.
[f] The average number of peroxide groups in the reactive LPA as measured by the iodine titration.[19]

The phase separation time (t_p) was recorded, the mixture was separated, and each layer was weighed.

Cure kinetics

For the cure kinetics study, 6–10 mg of the sample solution was placed in a hermetic aluminum sample pan. The isothermal reaction rate profile at 110°C was measured with a DuPont 9000 differential scanning calorimeter (TA Instruments, New Castle, DE), and the final conversion of total C═C bonds was calculated.[24]

Scanning electron microscopy (SEM)

In the morphological study, the fractured surface of the sample, which was cured at 110°c for 1 h followed by a postcure at 150°C for another 1 h in a stainless steel mold, was observed by SEM at 1000×.

Microvoids

The morphology of the sample during cure was also observed by means of an optical microscope. One drop of sample (ca. 0.8 mg) was placed between two microscope cover glasses, which were then inserted into a hot stage (Mettler, FP82HT, Columbus, OH). The cured sample at 110°C was chilled in liquid nitrogen and was subsequently observed at room temperature under an optical microscope with transmitted light at magnifications of 100–400×.

The quantity of microcracking in the morphology sample under an optical microscope was measured by means of an image analyzer.[7,11] Because the samples were of uniform thickness, the fraction of the image area, which was black (due to light scattering by the microcracks), was proportional to the volume of the microcracks in the sample.

Volume change and colorimetric measurements

Density measurements[11] at room temperature were used to obtain volume shrinkage data for isothermally cured specimens at 110°C, whereas measurements of color depth[17] at room temperature for the corresponding cured specimens were carried out with a chromameter (Minolta, CR-300, Tokyo, Japan). Ten measurements of the color depth index (L^*) were taken for both sides of the specimen, respectively. The higher the L^* value was, the lower the color depth was, and the hazing phenomenon of the cured specimen was more pronounced, which led to a lower internal pigmentability. In this study, an L^* value within 30 was recognizably dark red in tint and was used as the acceptable upper bound for good internal pigmentability.

RESULTS AND DISCUSSION

Synthesis of reactive LPAs

The reactivity of a synthesized LPA depends on the number of peroxide groups in its skeleton, which may be influenced by its reaction temperature history (Table I). In this work, the PPO ATPPO [see eq. (3)] was used as the initiator, whose half-life of thermal decom-

position [$t_{1/2}$ = 10 h at 61.3°C, as determined by differential scanning calorimetry (DSC) at a heating rate of 1.25°C/min and assuming first-order kinetics] exhibited similar activity to that of the conventional peroxides, such as lauroyl peroxide ($t_{1/2}$ = 10 h at 62°C) and benzoyl peroxide ($t_{1/2}$ = 10 h at 72°C)[25] for the initiation of vinyl monomer polymerization. In the synthesis of reactive LPAs, including PMMA and VAc-*b*-MMA, the peroxide linkages in the ATPPO and the PMMA segments were capable of thermal decomposition to generate free radicals during the 8-h reaction at 60–70°C. Therefore, either the higher the reaction temperature was or the longer the reaction time was, the smaller was the number of peroxide linkages that survived in the reactive LPA at the end of synthesis; this led to a less reactive LPA. For the reactive LPAs in this study, the average number of peroxide linkages per LPA molecule was 0.3–2.4 by the iodine titration method[19] (Table II).

For the VAc-*b*-MMA random block copolymer, the introduction of VAc altered the glass-transition temperature (T_g) and molecular polarity (μ') in comparison with PMMA. This may have then changed the miscibility of the ST/UP/LPA ternary system.

Characterization of ATPPO and LPA

Oshibe and Yamamoto[18] pointed out that the polycondensate ATCl obtained in eq. (1) is a mixture, poly(triethylene adipate)[A(TA)$_n$], with n ranging from 0 to 6. Their thin-layer chromatography and ^{1}H-NMR analysis showed that as n approached 1 [i.e., triethylene glycol-bis(adipoyl chloride) (ATA)], the weight distribution of the polycondensate reached a maximum. Therefore, the average molecular weight of the repeating unit for ATPPO in eq. (3) would be 404 g/mol if n was assumed to be 1. Because the M_n and weight-average molecular weight (M_w) of the ATPPO synthesized in this study were measured to be 5,000 and 12,800 g/mol by gel permeation chromatography (GPC), on average there were 12.4 peroxide groups in each
ATPPO molecule.

The molar compositions of the VAc-*b*-MMA types of LPAs, as shown in Table II, were identified by ^{1}H-NMR, where the peak intensities of —OCH$_3$ (δ = 3.4–3.6) for MMA and —O—CH < (δ = 4.0–4.2) for VAc were selected for the calculations. (A two-dimensional HETCOR experiment[26] of NMR was also carried out to confirm the peak assignment.)

M_n, as measured by GPC, for the eight reactive LPAs fell in the range of 18,000 to 136,000 g/mol, whereas the polydispersity (PD) ranged from 1.6 to 4.8 (Table II).

The DSC results in Table II show that the T_g values for PMMA were measured 96–102°C. For the VAc-*b*-MMA type of LPA, more than one T_g was measured for some of the systems [i.e., VAc-*b*-MMA38K(15) and VAc-*b*-MMA31K(24)], where the medium transition temperature (i.e., 75.9 or 65.5°C) was the T_g for the random block copolymer of VAc and MMA and where the lower (i.e., 46.4°C) and higher (i.e., 103.6 or 106.1°C) transition temperatures were the T_g for the PVAc and PMMA segments, respectively. The introduction of VAc monomer in the PMMA backbone led to a decrease in the stiffness of polymer chain and, in turn, a decrease in the T_g.

Compatibility of the ST/UP/LPA systems before curing

The μ' values of the UP resin and LPAs were evaluated in terms of the calculated dipole moment per unit volume[23] ($\mu/V^{1/2}$) with Debye's equation[27] and group contribution methods.[27,28] In general, the higher the polarity difference was per unit volume between the UP and LPA, the lower compatibility the compatibility was for the ST/UP/LPA system at 25°C before the reaction. The data in Table III reveal that among the eight reactive LPA systems, the sample solution containing VAc-*b*-MMA was theoretically more compatible than the PMMA systems. Also, for the sample solution containing the VAc-*b*-MMA type of LPA, the LPA with a higher content of VAc introduced may have led to a greater compatibility of the ST/UP/LPA system. [Theoretically, the VAc-*b*-MMA(24) system would have been the most compatible, whereas the VAc-*b*-MMA(14) system would have been the least compatible.] This was generally in agreement with the static phase characteristics data for the uncured ST/UP/LPA systems at 25°C (Table III), where the phase separation rate, as revealed by t_p, generally followed the same trend, with a longer t_p for the more compatible ST/UP/LPA ternary system.

Table III also shows this; for a fixed LPA (either PMMA or VAc-*b*-MMA with approximately the same amount of VAc content), a higher molecular weight of LPA generally resulted in a less compatible ST/UP/LPA system, as evidenced by a shorter t_p [cf. PMMA26K, PMMA57K, and PMMA136K systems; VAc-*b*-MMA18K(14) and VAc-*b*-MMA38K(15) systems; VAc-*b*-MMA26K(17) and VAc-*b*-MMA38K(15) systems; VAc-*b*-MMA31K(24) and VAc-*b*-MMA54K(24) systems]. This also confirmed by a higher degree of phase separation, as observed from a higher relative weight of the upper layer (w_u) when a higher molecular weight of LPA was added for the ST/UP/LPA system (except for the PMMA136K system).

The discrepancy for the PMMA136K system may be ascribed to the fact that in the calculation of μ' for the reactive LPA, the polar peroxide linkages (—R—CO—O—O—CO—R′—) in the backbone of the LPA was not taken into account. The higher molecular weight of LPAs such as PMMA136K then possessed a

TABLE III
Calculated V and μ Values for UP and LPA, Phase Characteristics for ST/UP/LPA Uncured Systems at 25 and 110°C, and α Values as Measured by DSC for ST/UP/LPA Systems Cured at 110°C

UP or LPA	μ	V	μ'	$\mu'_{UP} - \mu'_{LPA}$	$t_p(25)$	$w_u(\%)$	$t_p(110)$	α
Neat UP resin								
MA–PG–PA	3.13	1,389	0.0840		—			86.9
Reactive LPAs								
PMMA26K	10.48	21,290	0.0718	0.0122	495	14.7	>600	84.7
PMMA57K	15.50	46,680	0.0718	0.0122	341	48.2	>600	82.2
PMMA136K	23.95	111,400	0.0718	0.0122	135	13.3	>600	81.4
VAc-*b*-MMA18K(14)	8.80	14,640	0.0727	0.0113	650	14.7	>600	84.8[21]
VAc-*b*-MMA26K(17)	10.59	21,120	0.0729	0.0111	720	30.9	>600	82.1
VAc-*b*-MMA38K(15)	13.51	34,410	0.0728	0.0112	390	32.3	>600	80.0
VAc-*b*-MMA31K(24)	11.63	25,090	0.0734	0.0106	∞[a]	—	>600	83.5
VAc-*b*-MMA54K(24)	15.35	43,710	0.0734	0.0106	1025	41.3	>600	80.4
Nonreactive LPAs								
PVAc109K[20]	23.53	86,510	0.0800	0.0040	∞	—		73.0
VAc–VC16K(23)[21,22]	7.32	10,630	0.0710	0.0130	∞	—		76.0

μ = dipole moment (debye/mol$^{1/2}$); V = molar volume (cm^3/mol); μ' = dipole moment per unit volume [$(\mu^2/V)^{1/2}$ (debye/cm$^{3/2}$)]; t_p = phase separation time (min) at 25°C [i.e., $t_p(25)$] and 110°C [i.e., $t_p(110)$]; w_u = weight percentage for the upper-layer solution after a phase equilibrium at 25°C (%); α = cure conversion of total C═C bonds (%) for ST/UP/LPA systems as measured by DSC at 110°C.

[a] One phase μ'_{UP} and μ'_{LPA} are dipole moments per unit volume for UP and LPA, respectively.

higher μ' than that shown in Table III, which may have led to a lower degree of phase separation for the ST/UP/LPA system, as compared with the PMMA26K and PMMA57K systems, despite its faster phase separation rate.

As the mixing temperature was increased from 25 to 110°C, no phase separation was observed for all eight ST/UP/LPA ternary systems within 600 min (Table III), after which they started to polymerize despite no addition of the TBPB initiator in the system (the reactive LPAs possessed peroxide linkages at their backbones though). As shown later, for the ST/UP/LPA system with the initiator TBPB, the reaction at 110°C isothermally ended in 80 min. Therefore, all eight systems in this study exhibited a single homogeneous phase after a phase equilibrium before the reaction at 110°C.

The higher the mixing temperature was, the more compatible was the ST/UP/LPA ternary system containing reactive PMMA as an LPA over the temperature range of 25–110°C, as evidenced by a longer t_p (135–495 min vs at least 600 min). Hence, the ST/UP/LPA ternary system containing a relatively nonpolar reactive PMMA as an LPA in this study possessed an upper critical solution temperature instead of a lower critical solution temperature.

Cured sample morphology, cure kinetics, and compatibility of cured ST/UP/LPA ternary systems

For the ST/UP/LPA sample solution containing PMMA, the addition of a higher molecular weight of LPA led to a more pronounced phase separation phenomenon during curing at 110°C, where the PMMA26K system exhibited a homogeneous globule morphology [Fig. 1(a)] and where the PMMA57K [Fig. 1(b)] and the PMMA136K [Fig. 1(c)] systems possessed a two-phase microstructure consisting of a flake-like continuous phase and a globule dispersed phase.

For the ST/UP/LPA sample solutions containing VAc-*b*-MMA with a molar composition of 15% VAc (i.e., the VAc-*b*-MMA18K(14), VAc-*b*-MMA26K(17), and VAc-*b*-MMA3 8K(15) systems), the addition of a higher molecular weight of LPA led to a more pronounced phase separation phenomenon, where the VAc-*b*-MMA18K(14) system exhibited a homogeneous globule morphology [Fig. 1(d)] and where the VAc-*b*-MMA26K(17) system possessed a two-phase microstructure consisting of a continuous phase and a globule dispersed phase [Fig. 1(e)]. Further increasing the molecular weight of LPA [i.e., the VAc-*b*-MMA38K(15) system in Fig. 1(f)] resulted in a less severe phase separation, which could be due to a decrease in the phase separation rate caused by the increase in the viscosity for the ST/UP/LPA system during curing.

For the ST/UP/LPA sample solutions containing VAc-*b*-MMA with a molar composition of 24% VAc [i.e., the VAc-*b*-MMA31K(24) and the VAc-*b*-MMA54K(24) systems], the addition of a higher molecular weight LPA led to a more pronounced phase separation phenomenon, where the VAc-*b*-MMA31K(24) system exhibited a homogeneous globule morphology [Fig. 1(g)], whereas the VAc-*b*-MMA54K(24) system possessed a two-phase microstructure consisting of a flake-like continuous phase and a globule dispersed phase [Fig. 1(h)].

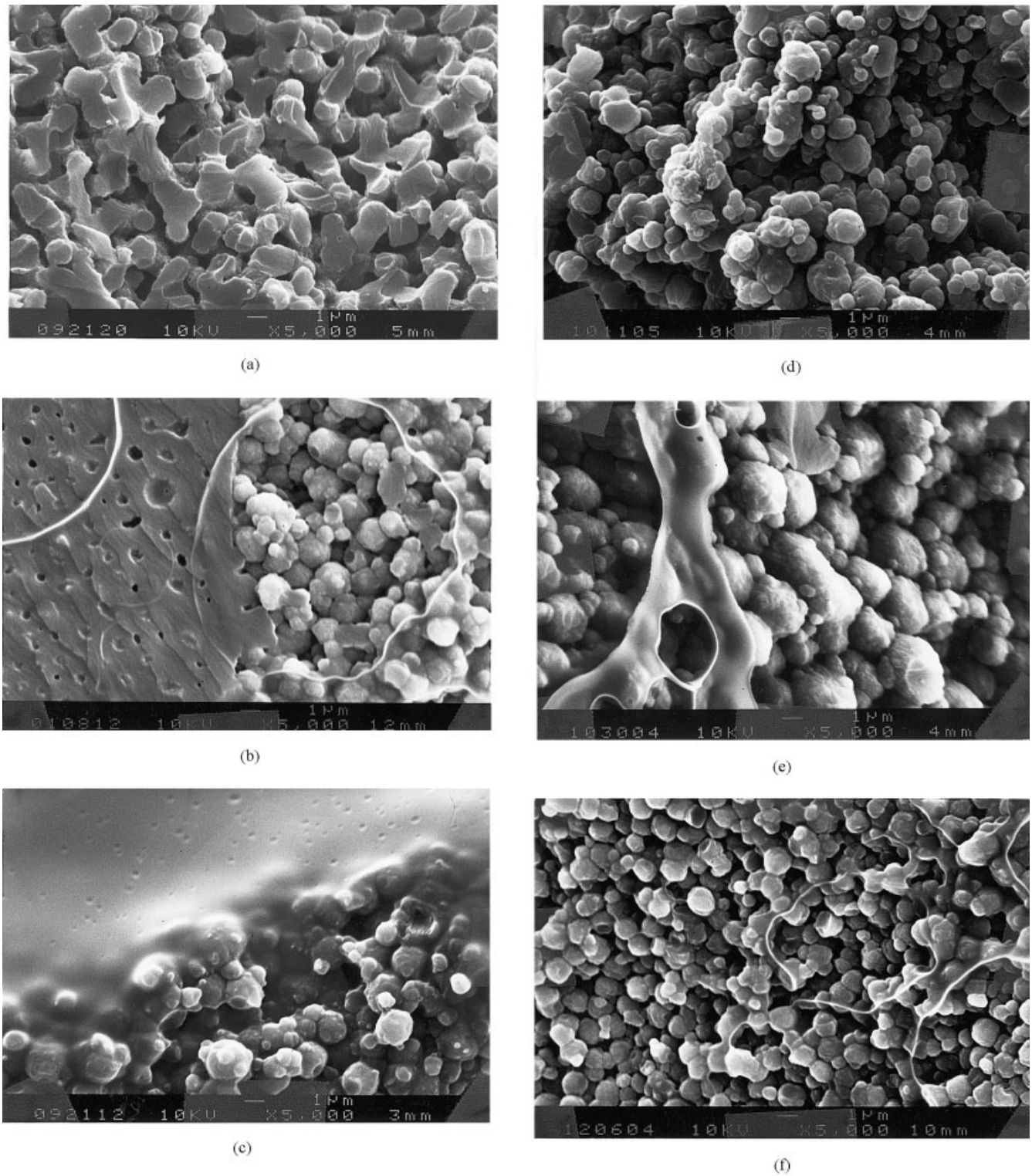

Figure 1 Effects of LPA types on the cured sample morphology under SEM: (a) PMMA26K, (b) PMMA57K, (c) PMMA136K, (d)VAc-*b*-MMAI8K(14), (e) VAc-*b*-MMA26K(17), (f) VAc-*b*-MMA38K(15), (g) VAc-*b*-MMA31K(24), (h) VAc-*b*-MMA54K(24), (i) PVAc109K, and (j) VAc–VC16K(23).

For the ST/UP/LPA sample solution containing PMMA, the isothermal DSC rate profiles at 110°C (Fig. 2) showed that the addition of a higher molecular weight LPA (i.e., the more incompatible ST/UP/LPA ternary system) led to a later onset of the cure reaction. Also, a relatively lower peak reaction rate resulted, which was an indication of a less compatible ternary system.[20] This may support the trend of the compati-

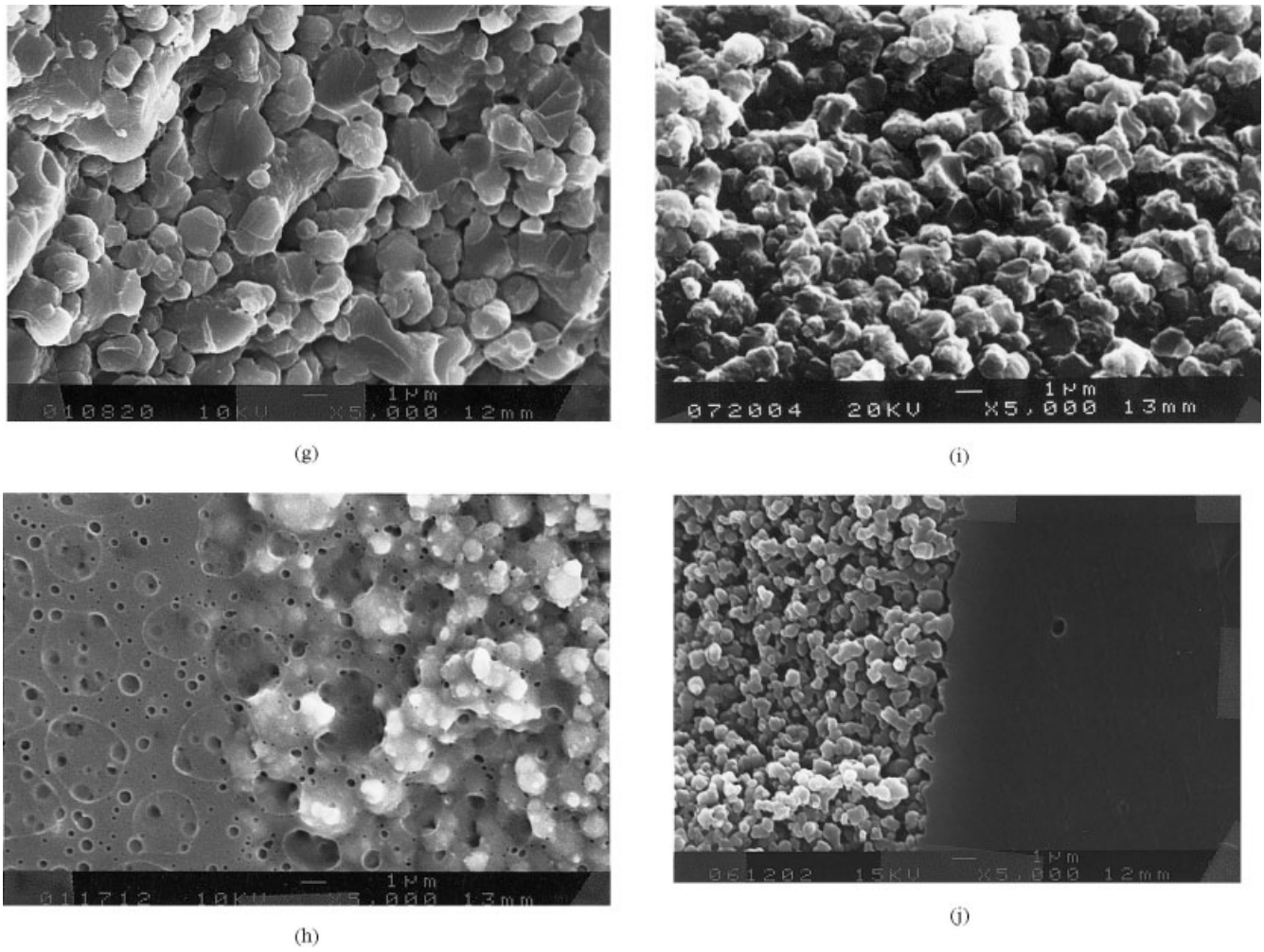

Figure 1 *(Continued)*

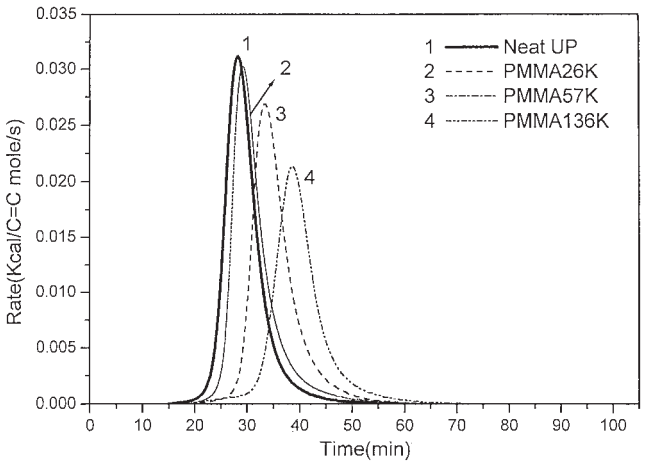

Figure 2 Effects of the reactive PMMA types of LPA on the DSC reaction rate profile at 110°C for the ST/UP/LPA systems.

bility of the cured ST/UP/LPA systems as revealed by the SEM micrographs in Figure 1(a–c) (i.e., PMMA26K > PMMA57K > PMMA136K). The final conversion of the total C═C bonds, as measured by DSC (Fig. 3), showed that the addition of a LPA may have led to a reduction in the cure conversion when compared with that of the neat UP resin. Also, the more incompatible the ST/UP/LPA system was, the lower the final conversion was (i.e., PMMA26K > PMMA57K > PMMA136K).

For the ST/UP/LPA sample solution containing VAc-*b*-MMA, the isothermal DSC rate profiles at 110°C (Fig. 4) showed that with a molar composition of 15% VAc in the LPA [i.e., the VAc-*b*-MMA26K(17) and VAc-*b*-MMA38K(15) systems], the addition of a higher molecular weight of LPA led to an earlier onset of the cure reaction and a relatively higher peak reaction rate. The latter indicates that the VAc-*b*-MMA26K(17) system was less compatible than the VAc-*b*-MMA38K(15) system during curing, which agreed with the SEM results shown in Figure 1(e,f). However, the DSC cure conversion was lower for the

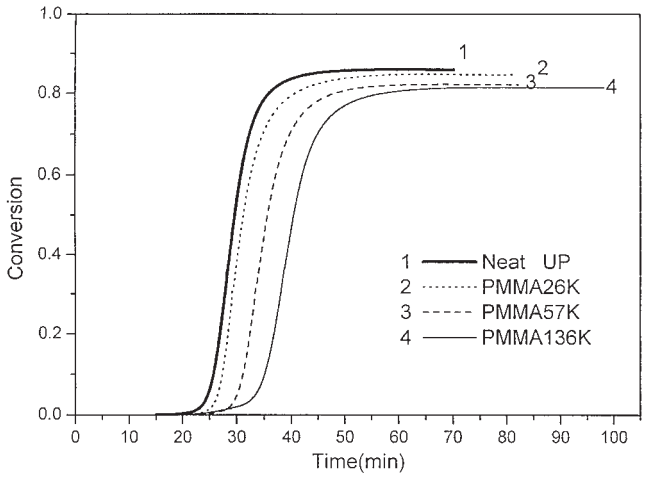

Figure 3 Effects of the reactive-PMMA-type LPAs on the DSC conversion profile at 110°C for the ST/UP/LPA systems.

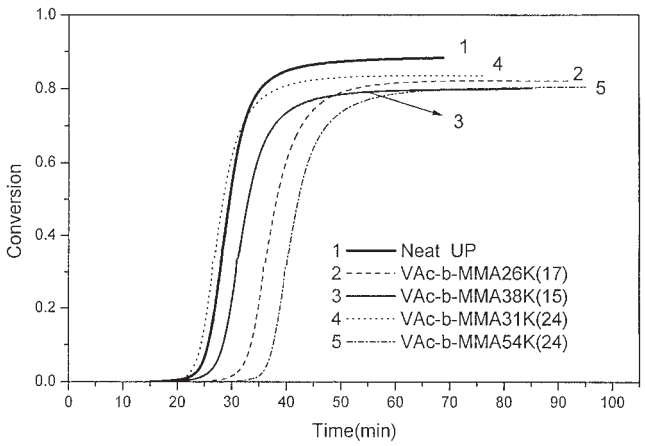

Figure 5 Effects of the reactive VAc-*b*-MMA types of LPA on the DSC conversion profile at 110°C for the ST/UP/LPA systems.

more compatible VAc-*b*-MMA38K(15) system (Fig. 5). In contrast, for the VAc-*b*-MMA31K(24) and VAc-*b*-MMA54K(24) systems with molar composition of 24% VAc introduced in the LPA, the VAc-*b*-MMA54K(24) system was less compatible as revealed by SEM, yet it did not exhibit a lower DSC peak reaction rate. Rather, it possessed a later onset of the curing reaction, a broader DSC rate profile (an indication of the lower compatibility of the ST/UP/LPA system), and a lower DSC cure conversion.

Relationship between the morphologies and mechanical properties: The Takayanagi models

For the cured LPA-containing UP resin systems with their characteristic morphologies, as shown in Figure 1(a–j), the mechanical behaviors could be approximately represented by the Takayanagi models,[29,30] where arrays of weak LPA (R) and stiff ST-crosslinked polyester (P) phases were indicated (Fig. 6). The subscripts 1, 2, and 3 for the P phases are used to distinguish the ST and UP compositions as a result of phase separation during curing, and the quantities λ, ϕ, ξ, and ν or their indicated multiples indicate the volume fractions of each phase.

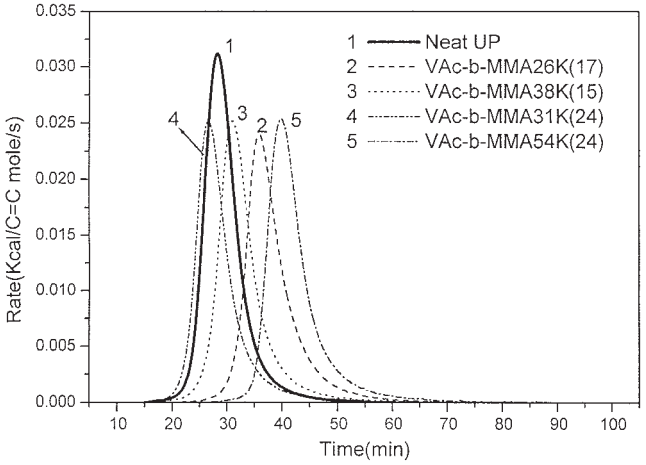

Figure 4 Effects of the reactive VAc-*b*-MMA types of LPA on the DSC reaction rate profile at 110°C for the ST/UP/LPA systems.

For the systems shown in Figure 1(a,d,g,i), the microgel particles (phase P_1) were surrounded by a layer of LPA (phase R). Between the LPA-covered microgel particles, there were some lightly ST-crosslinked polyester chains and PS chains (taken both together as phase P_2), with different compositions of ST and UP from those in phase P_1 dispersed in the LPA phase (phase R). Hence, the characteristic globule microstructure may be represented by the P–P–S model, as shown in Figure 6(a), which is a parallel combination of the three elements, that is, P_1, R, and P_2–R in series. In contrast, for the system shown in Figure 1(b,c,e,f,h,j), the microstructure consisted of a stiff continuous phase of ST-crosslinked polyester (phase P_1) and a weak globule LPA-dispersed phase, whose globule morphology could also be represented by a P–P–S model. Hence, the upper bound of mechanical behavior for the overall morphology could be represented by a P–(P–P–S) model, as shown in Figure 6(b), which is simply a parallel combination of the continuous phase P_1 and the dispersed phase denoted by a P–P–S model.

Volume shrinkage and internal pigmentability

The volume shrinkage of the neat UP resin was about 8.4%, whereas the addition of different reactive PMMA and VAc-*b*-MMA types of LPAs could generally reduce the volume shrinkage to about −8 to 5%

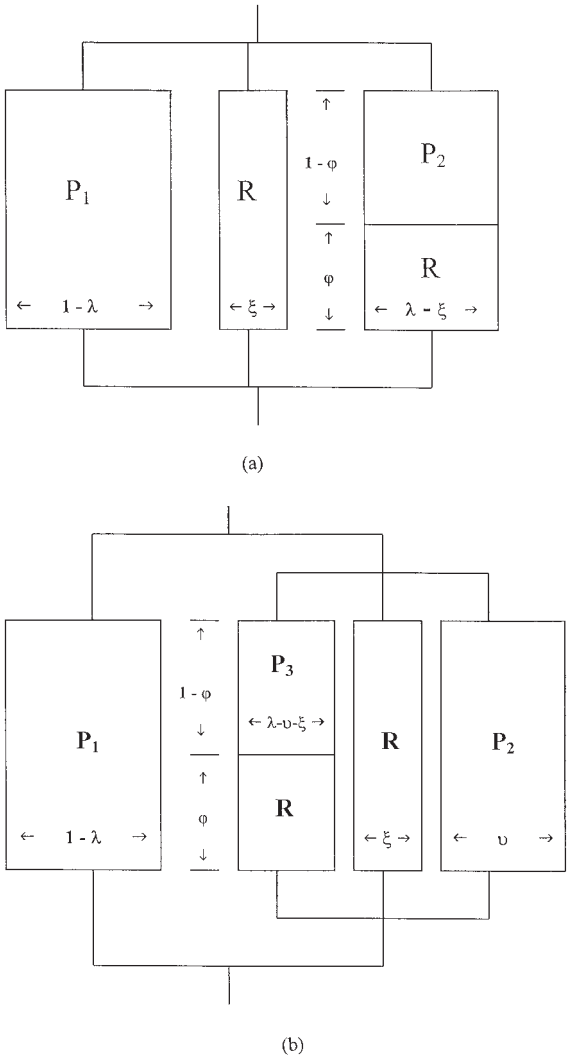

Figure 6 Takayanagi models for the mechanical behavior of cured LPA-containing UP resin systems: (a) P–P–S and (b) P–(P–P–S) models. The area of each diagram is proportional to a volume fraction of the phase.

(expansion; Table IV). For the ST/UP/LPA systems containing reactive PMMA as an LPA, the most compatible PMMA26K system showed a volume expansion after curing (the fractional volume change, $\Delta V/V_0$ = 5.4%), whereas the addition of a higher molecular weight of LPA resulted in a greater volume shrinkage. Similarly, for the VAc-*b*-MMA systems, the most compatible VAc-*b*-MMA18K(14) system was the most effective for the volume shrinkage control ($\Delta V/V_0$ = −1.0%), whereas the addition of a higher molecular weight of LPA (under approximately the same level of VAc content introduced in the LPA) led to a greater volume shrinkage (Table IV).

Except for the VAc-*b*-MMA26K(17) and VAc-*b*-MMA31K(24) systems, the effects of the LPA chemical structure on the L^* value as the index of internal pigmentability for the ST/UP/LPA systems after curing generally showed a trend reverse to those on the fractional volume shrinkage. (The higher the L^* value was, the worse the internal pigmentability was.) Because an L^* value within about 30 could be used as the acceptable upper bound for good internal pigmentability in this study, except for the PMMA26K, VAc-*b*-MMA26K(17), and VAc-*b*-MMA31K(24) systems, the other five systems exhibited good internal pigmentability (Table IV).

Effects of microvoid formation on volume shrinkage

Pattison et al.[5,6] proposed that as the crosslinking of LPA-containing UP resins proceeds, strain due to polymerization shrinkage develops in the system, particularly at the interface of the LPA phase (phase R) and the crosslinked UP phase (phase P). This strain could increase to the point that stress cracking propagates

TABLE IV
Volume Shrinkage Data ($\Delta V/V_0$), L^* Values as the Index of Internal Pigmentability for Both Sides of the Molded Parts, and v_m Values for the ST/UP/LPA Systems After Isothermal Curing at 110°C

LPA added	$\Delta V/V_0$ (%)	L^* (upper side)[a]	L^* (bottom side)[a]	v_m (%)
Neat UP resin	−8.41	22.53 (0.03)[a]	23.19 (0.05)	—
Reactive LPAs				
PMMA26K	+5.43	39.06 (0.21)	30.16 (0.09)	12.26
PMMA57K	−7.87	26.61 (0.03)	25.34 (0.04)	11.05
PMMA136K	−8.11	24.06 (0.21)	23.38 (0.15)	10.77
VAc-*b*-MMA18K(14)	−0.99	26.85 (0.05)	30.35 (0.20)	3.84
VAc-*b*-MMA26K(17)	−7.24	45.14 (0.17)	26.32 (0.07)	3.06
VAc-*b*-MMA38K(15)	−7.43	23.31 (0.03)	25.41 (0.03)	2.12
VAc-*b*-MMA31K(24)	−7.85	36.32 (0.66)	28.42 (0.32)	1.75
VAc-*b*-MMA54K(24)	−7.96	26.28 (0.66)	24.19 (0.05)	1.36
Nonreactive LPAs				
PVAc109K[20]	−2.1	24.94 (0.06)	24.93 (0.08)	48.97
VAc–VC16K(23)[21,22]	−3.5	24.23 (0.06)	25.85 (0.08)	31.39

[a] The values in parentheses represent the estimated standard errors for the experimental averages.

through the weak LPA phase, relieving this strain, forming microcracks and/or microvoids, and compensating for the overall volume shrinkage by the microcrack or microvoid space. However, for the ST/UP/LPA systems containing reactive LPAs, the data for the relative volume fraction of microvoids (v_m) shown in Table IV do not fully explain the experimental results, where the system with a smaller v_m, such as the VAc-*b*-MMA18K(14) system, did not necessarily have a higher volume shrinkage and vice versa. This was in contrast to the ST/UP/LPA system containing nonreactive LPAs, such as PsVAc109K and VAc–VC (vinyl chloride) 16K(23), which led to a higher relative v_m (31–49%) and, in turn, a good volume shrinkage control ($\Delta V/V_0 = -2.1$ to -3.5%; see Table IV).

Effects of microvoid formation on internal pigmentability

Microvoid formation is intimately connected with internal pigmentability.[17] As incident light entered an internally pigmented part of the cured ST/UP/LPA system, the intensity of reflective light of the pigment could be greatly reduced due to the severe light scattering, which may have occurred at the solid/air (microvoid) interface inside the parts, leading to the hazing of a pigment's color. In theory, the higher the v_m is, the worse the internal pigmentability will be. However, for the ST/UP/LPA systems containing reactive LPAs, the relative v_m data shown in Table IV could not fully explain the experimental results, where systems with a smaller v_m, such as the VAc-*b*-MMA26K(17) and VAc-*b*-MMA31K(24) systems, did not necessarily lead to a better internal pigmentability (i.e., a lower L^* value).

Effects of intrinsic polymerization on volume shrinkage

Besides microvoid formation, the intrinsic polymerization shrinkage is also important in the determination of the volume shrinkage control during the curing of the ST/UP/LPA systems. On the basis of our experimental data from the SEM micrographs, the reactive LPAs with lower molecular weights, such as PMMA26K and VAc-*b*-MMAI8K(14), led to expansion effects on the ST-crosslinked polyester microgel structure [see Fig. 1(a,d)], which were caused by the reduction in the cyclization reaction of the UP resin during curing (due to the intermolecular reaction between UP and reactive LPA) and the repulsive forces between chain segments of UP and LPA within the microgel structures, and a lower intrinsic polymerization shrinkage resulted (see Fig. 7).

In the design of reactive PMMA-*b*-PVAc types of LPAs, the less polar PMMA segment, with peroxide linkages on it, was reactive, whereas the more polar

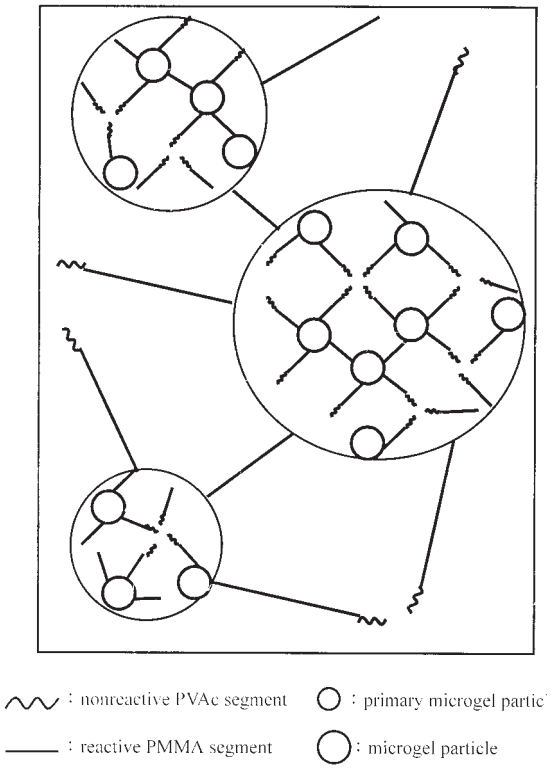

Figure 7 Schematic diagram showing the expansion effect of reactive LPA on the microgel structure during the curing of the ST/UP/LPA systems.

PVAc segment was nonreactive. In the subsequent curing of the ST/UP/LPA system, the ST-crosslinked polyester microgel particles, with the less polar PMMA segment of the LPA covalently bonded to their surfaces, tended not to overlap with each other (see Fig. 7) due to the incompatibility between UP and PMMA and could thus facilitate the reduction of polymerization shrinkage due to the expansion effect of the microgel structure. [The microgel structure (large circle in Fig. 7) was composed of tens and hundreds of primary microgel particles (small circle in Fig. 7) with unsaturated C═C double bonds at their surfaces.]

This expansion effect hence depended on three factors, namely, the repulsive forces between the chain segments of UP and LPA, the reactivity of LPA (i.e., average number of peroxide groups in the LPA backbone), and the LPA molecular weight. This was the reason the VAc-*b*-MMA18K(14) system, with a relatively small v_m (≈4%), led to a very good volume shrinkage control.

Factors in good volume shrinkage control and acceptable internal pigmentability

Either a higher v_m or a lower intrinsic polymerization was required for good volume shrinkage control for the ST/UP/LPA systems. The nonreactive PVAc109K

and VAc–VC16K(23) systems pertained to the former case, whereas the reactive VAc-*b*-MMA18K(14) system was categorized as the latter case (Table IV).

In addition to the v_m, the average size of microvoids were also influential on the internal pigmentability. For the PMMA26K, VAc-*b*-MMA26K(17), and VAc-*b*-MMA31K(24) systems, we inferred that the average size of microvoids generated during curing was close to the wavelength of visible light (λ = 0.45–0.75 μm), where the light scattering at the solid/air (microvoid) interface was more pronounced and led to a lower internal pigmentability.

Among the eight ST/UP/LPA systems containing reactive LPAs, the VAc-*b*-MMAI8K(14) system provided a very good volume shrinkage control ($\Delta V/V_0$ = −1.0%) and achieved acceptable internal pigmentability ($L^* \cong$ 26–30). Despite its relatively lower v_m ($\approx$4%), we inferred that the average size of the microvoids was smaller than 0.05–0.1 μm, which was about 1/10 to 1/5 of the wavelength of visible light, so the light scattering caused by the microvoids was insignificant, and the haziness of a pigment's color was minimized.

CONCLUSIONS

For ST/UP/LPA systems, microvoid formation could affect both the volume shrinkage control and the internal pigmentability for the cured sample. A higher v_m was favorable for the reduction of volume shrinkage, whereas a smaller average size of microvoids, as compared with 0.45–0.75 μm for the wavelength of visible light, was indispensable for an acceptable pigmentability in the cured samples.

In addition to microvoid formation, the intrinsic polymerization shrinkage was also important in the determination of the volume shrinkage control during the curing of the ST/UP/LPA system. The intrinsic polymerization shrinkage could be reduced through the use of reactive PMMA and PVAc-*b*-PMMA types of LPA with peroxide groups in their backbone, which led to expansion effects on microgel structures during curing. This was ascribed to the reduction in the cyclization of the UP resin during curing, caused by the intermolecular reaction between UP and reactive LPA and to the repulsive forces between chain segments of UP and LPA within the microgel structures. In this study, the use of a MA–PG–PA type of UP resin (molar ratio of MA/PA $\cong$ 0.63 : 0.37) and a reactive VAc-*b*-MMA18K(14) type of LPA (M_n = 18,000 g/mol, T_g = 92.7°C, and molar ratio of VAc/MMA $\cong$ 0.14 : 0.86) under isothermal curing at 110°C) led to very good volume shrinkage control ($\Delta V/V_0 \cong = -1.0\%$) and acceptable pigmentability ($L^* \cong$ 26–30) for the molded parts.

References

1. Bartkus, E. J.; Kroekel, C. H. Appl Polym Symp 1970, 15, 113.
2. Yang, Y. S.; Lee, L. J. Polymer 1988, 29, 1793.
3. Goosey, M. T. In Plastics for Electronics; Goosey, M. T., Ed.; Elsevier: New York, 1985; Chapter 4, p 101.
4. Atkins, K. E. In Sheet Molding Compounds: Science and Technology; Kia, H. G., Ed.; Hanser: New York, 1993; Chapter 4.
5. Pattison, V. A.; Hindersinn, R. R.; Schwartz, W. T. J Appl Polym Sci 1974, 18, 2763.
6. Pattison, V. A.; Hindersinn, R. R.; Schwartz, W. T. J Appl Polym Sci 1975, 19, 3045.
7. Mitani, T.; Shiraishi, H.; Honda, K.; Owen, G. E. Proceedings of the 44th Annual Conference, Cincinnati, OH; SPI Composites Institute: New York, 1989; p 12F.
8. Suspene, L.; Fourquier, D.; Yang, Y. S. Polymer 1991, 32, 1593.
9. Hsu, C. P.; Kinkelaar, M.; Hu, P.; Lee, L. J. Polym Eng Sci 1991, 31, 1450.
10. Bucknall, C. B.; Partridge, I. K.; Phillips, M. J. Polymer 1991, 32, 636.
11. Huang, Y. J.; Liang, C. M. Polymer 1996, 37, 401.
12. Li, W.; Lee, L. J. Polymer 2000, 41, 697.
13. Zhang, Z.; Zhu, S. Polymer 2000, 41, 3861.
14. Nippon Oil and Fats Corp. U.S. Pat. 4,303,762 (1981).
15. Fukushi, K.; Moriya, Y.; Yamamoto, T. Kobunshi Ronbunshu 1987, 44, 97.
16. Ujikawa, U.; Takamura, M.; Laurent, F. B.; Bucknall, C. B. Proceedings of International Composite EXPO'97, Nashville, TN; SPI Composites Institute: New York, 1997; p 22C.
17. Atkins, K. E.; Rex, G. C.; Reid, C. G.; Seats, R. L.; Candy, R. C. Proceedings of the 47th Annual Conference, Cincinnati, OH; SPI Composites Institute: New York, 1992; p 7D.
18. Oshibe, Y.; Yamamoto, T. Kobunshi Ronbunshu 1987, 44, 73.
19. Suzuki, N.; Moriya, Y.; Yamamoto, T Kobunshi Ronbunshu 1987, 44, 81.
20. Huang, Y. J.; Chen, T. S.; Huang, J. G.; Lee, F. H. J Appl Polym Sci 2003, 89, 3336.
21. Twu, I. B. M.S. Thesis, National Taiwan University of Science and Technology, 2000.
22. Huang, Y. J.; Dong, J. P.; Yang, J. J.; Lee, J. H.; Lai, D. H. Polym Mater Sci Eng 2001, 85, 497.
23. Huang, Y. J.; Jiang, W. C. Polymer 1998, 39, 6631.
24. Huang, Y. J.; Su, C. C. J Appl Polym Sci 1995, 55, 305.
25. Pastorino, R. L. In Unsaturated Polyester Technology; Bruins, P. F., Ed.; Gordon and Breach: New York, 1976; p 65.
26. Pavia, D. L.; Lampman, G. M.; Kriz, G. S. Introduction to Spectroscopy: A Guide for Students of Organic Chemistry, 3rd ed.; Harcourt: Philadelphia, 2001; p 545.
27. Krevelen, D. W. V. Properties of Polymers, 3rd ed.; Elsevier: London, 1990; pp 198, 323.
28. Fendor, R. F. Polym Eng Sci 1974, 14, 147.
29. Takayanagi, M.; Imada, K.; Kajiyama, T. J Polym Sci Part C: Polym Symp 1966, 15, 263.
30. Huang, Y. J.; Horng, J. C. Polymer 1998, 39, 3683.